# Cellulose phosphorylation comparison and analysis of phosphorate position on cellulose fibers

Fleur Rol, Cécile Sillard, Michel Bardet, Jayasubba Reddy Yarava, Lyndon Emsley, Corinne Gablin, Didier Léonard, Naceur Belgacem, Julien Bras

# Cellulose phosphorylation optimization and analysis of phosphorus position on cellulose fibers

Fleur Rol [a], Cécile Sillard [a], Michel Bardet[c,d], Jayasubba Reddy Yarava [c], Lyndon Emsley[c]
Corinne Gablin[e], Didier Léonard[e], Naceur Belgacem [a], Julien Bras*[,a,b]

[a] Univ. Grenoble Alpes, CNRS, Grenoble INP, LGP2, F-38000 Grenoble, France
[b] Institut Universitaire de France (IUF), F-75000 Paris, France
[c] Institut des Sciences et Ingénierie Chimiques, Ecole Polytechnique Fédérale de Lausanne (EPFL), CH-1015 Lausanne, Switzerland
[d] Université Grenoble Alpes, CEA, INAC, MEM, Laboratoire de Résonance Magnétique, Grenoble, 38000, France
[e] Univ Lyon, CNRS, Université Claude Bernard Lyon 1, ENS de Lyon, Institut des Sciences Analytiques, UMR 5280, 5, rue de la Doua, F-69100 Villeurbanne, France

Email adresses :
Fleur.rol@grenoble-inp.fr
Cecile.sillard@lgp2.grenoble-inp.fr
Michel.bardet@cea.fr
yarava@fmp-berlin.de
lyndon.emsley@epfl.ch
Corinne.gablin@isa-lyon.fr
Didier.leonard@isa-lyon.fr
Naceur.belgacem@grenoble-inp.fr
Julien.bras@grenoble-inp.fr

*Corresponding author
Julien Bras: julien.bras@grenoble-inp.fr
LGP2
461 rue de la papeterie
38402 Saint Martin d'Hères
France
+33 (0)4 76 82 69 15

**Keywords:** phosphorylation, cellulose, NMR, ToF-SIMS

## Highlights

- Cellulose phosphorylation was studied in order to improve the final charge content
- The effect of phosphate salt constant of solubility was studied
- The position and penetration of the phosphate groups on the fibers were evaluated

**Abstract.** Chemical modifications of cellulose fibers as pretreatment for cellulose nanofibrils (CNF) production have been investigated to improve the production process and the quality of obtained cellulosic nanomaterial. In this study, phosphorylation of cellulose fibers was optimized in anticipation of a future nanofibrillation. Different phosphate salts, namely $NH_4H_2PO_4$, $(NH_4)_2HPO_4$, $Na_2HPO_4$, $NaH_2PO_4$ and $LiH_2PO_4$ with different constants of solubility (Ks) were used to increase the efficiency of the modification. Phosphorylated cellulose pulps were analyzed using elemental analysis, solid-state $^{13}C$ and $^{31}P$ NMR, or conductimetric titration method. No effect of Ks was observed whereas a counterion effect was pointed out. The study also reported the effect of pH, cellulose concentration, temperature and urea content in phosphorylation efficiency. Finally, chemical functionalization and penetration of phosphorus in the cellulose fibers were evaluated using XPS, SEM-EDX, ToF-SIMS and solid-state NMR.

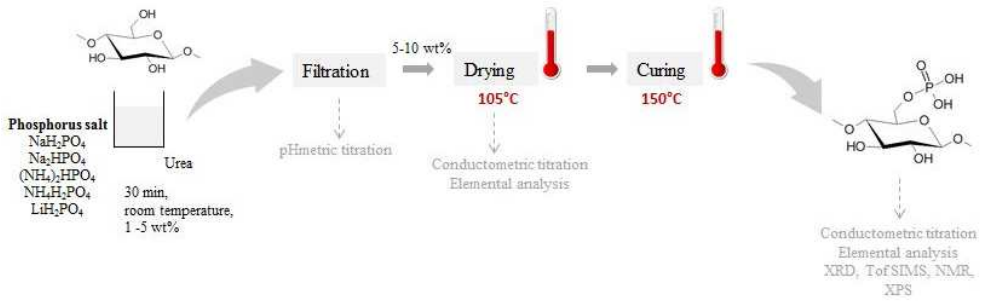

## 1. Introduction

Cellulose, the most abundant polymer on Earth, can be nanofibrillated since 1980. Cellulose nanofibrils (CNF) are described in many books and reviews (Dufresne, 2013; Klemm et al., 2011; Lavoine, Desloges, Dufresne, & Bras, 2012; Rol, Belgacem, Gandini, & Bras, 2018). They are sustainable, biodegradable and biocompatible materials. CNF films are transparent, barrier and with high mechanical properties which make them useful in many applications such as packaging (Lavoine et al., 2012; Saini, Yücel Falco, Belgacem, & Bras, 2016), paper (Patent No. WO 2014118466 (A1), 2014; Brodin, 2014) or nanocomposites. However, the use of CNF is still limited due to the high energy consumption during the production. To overcome this issue, chemical pretreatments of cellulose fibers are used since 2000's to weaken the hydrogen bonds between fibers, and make the nanofibrillation easier. Moreover, CNF produced via a chemical pretreatment usually present better homogeneity and/or new functionalities as recently reviewed (Rol et al., 2018). TEMPO (2,2,6,6-Tetramethylpiperidine 1-oxyl) oxidized CNF(Isogai, Saito, & Fukuzumi, 2011) are classically produced and present higher quality mainly due to their charges which create repulsion and facilitate the nanofibrils liberation. Cationic CNF can also be produced via cellulose fibers reaction with EPTMAC (2,3-Epoxypropyl)trimethylammonium chloride). In this case, they display antimicrobial properties thanks to the amine quaternary grafted (Chaker & Boufi, 2015; Littunen et al., 2016; Saini et al., 2016). However, the main drawback of those classic chemical pretreatments resides in the use of toxic chemicals and complex procedures still difficult to industrialize.

Since 2013, new pretreatments have been developed in order to further increase the quality, with low energy consumption, produce greener CNF and impart new properties. For example, Ghanadpour et al. (Ghanadpour, Carosio, Larsson, & Wågberg, 2015) introduced negative charges on cellulose fibers thanks to the phosphorylation. Sulfite softwood pulp was impregnated with ammonium hydrogen phosphate and urea at 1 wt%, filtered to a solid content of 10 wt%, dried at 70°C and then cured at 150°C. Maximal charge of 1,8 mmol/g was measured and CNF of high quality with flame-retardant properties were produced via a microfluidizer. Phosphorylation of cellulose fibers for nanofibrillation is a very recent process which can lead to high-quality CNF, easily produced at industrial scale. Today, few publications are available. Naderi et al. (Naderi et al., 2016), used similar protocol without filtration step and using $NaH_2PO_4$. They showed that microfluidization is impossible under a degree of substitution of 0.13. Another protocol was proposed in 2017 by Noguchi et al. (Noguchi, Homma, & Matsubara, 2017) and allows reaching a charge content of 2.2 mmol/g.

Softwood pulp sheets were soaked in solution of $NH_4H_2PO_4$ and urea and then cured in hot air at 165°C for 10 min. CNF of 3-4 nm wide and high transparency suspensions were produced thanks to a homogenizer. The phosphorylation does not lead in change in crystallinity or degree of polymerization (DP) of the cellulose fibers. Such good results have been even transfer to industry with first production announcement in Japan (Yajima, 2018).

Even if phosphorylated CNF have appeared recently, cellulose phosphorylation is an old and well-known process. Phosphorylated cellulose is used in many fields as for example orthopaedics (Petreus et al., 2014), biomedical (Granja et al., 2001; Mucalo, Kato, & Yokogawa, 2009), textiles (Davis, Findlay, & Rogers, 1949) or bio-chemical separation (Suflet, Chitanu, & Popa, 2006). Phosphate groups can be introduced to cellulose during homogeneous or heterogeneous reaction. In many papers, cellulose phosphorylation is done on organic solvent such as pyridine (Reid & Mazzeno, 1949; Reid, Mazzeno, & Buras, 1949) or dimethylformamide (Katsuura & Mizuno, 1966) using phosphorylating agents such as phosphorus pentoxide, phosphoric acid or phosphate salt (Aoki & Nishio, 2010; Coleman et al., 2011; Inagaki, Nakamura, Asai, & Katsuura, 1976; Reid et al., 1949). Microcrystalline cellulose was also phosphorylated in molten urea as solvent using phosphorus acid (Suflet et al., 2006). Cellulose can also be phosphorylated using water, urea and phosphoric acid/salts. For example, Gallagher (Gallagher, 1965) soaked cotton fibers in phosphate salt solution before heating at a temperature superior to 100°C for less than 15 min. Ichiwaka et al. (Patent No. JP54138060A, 1979) used almost the same protocol but the curing step was longer (1-3h) for obtaining fire retardant materials. Nuessle et al. (Nuessle, Ford, Hall, & Lippert, 1956) phosphorylated cellulose by immerging fibers in a water/urea/diammonium phosphate system followed by a curing step at 150°C for 10 min. In many papers, urea is used to enhance fiber swelling and to prevent the degradation of cellulose during the curing step. Phosphorylation of cellulose fibers in water based urea system using phosphate salts appears as the easier process and it is the one classically used to produce CNF (Ghanadpour et al., 2015; Naderi et al., 2016; Noguchi et al., 2017). However, only few papers tried to optimize this process and understand the role of salts solubility parameter, their penetration and functionality.

The aim of this work is to optimize the phosphorylation of cellulose fibers in aqueous media to increase the phosphorus content. For that, adsorption of different phosphate salts on cellulose fibers was studied and phosphate salts with different constants of solubility were tested. Position of phosphate group on the anhydroglucose unit and phosphorus penetration on the fibers were also studied using ToF-SIMS, NMR and SEM-EDX.

## 2. Materials & methods

### 2.1 Materials

Cellulose used throughout this work is eucalyptus bleached kraft pulp Fibria T35. All the materials and chemicals were used as received from the producers: urea (99.5%, Roth), ammonium phosphate monobasic ($NH_4H_2PO_4$, >99%, Sigma Aldrich), ammonium phosphate dibasic ($(NH_4)_2HPO_4$, >99%, Sigma Aldrich), lithium phosphate monobasic ($LiH_2PO_4$, 99%, Sigma Aldrich), sodium phosphate monobasic ($NaH_2PO_4$, >99%, Sigma Aldrich), sodium phosphate dibasic ($Na_2HPO4$, 99%, Sigma Aldrich), sodium hydroxide (NaOH, 99%, Sigma Aldrich), hydrochloric acid (HCl, 37%, Sigma Aldrich). Distilled water was used for all the preparations.

### 2.2 Methods

*Refining cellulose.* Cellulose fibers were dispersed in water at 2 wt% and refined using a pilot disk beater (Matech, France) until reaching a Schopper-Riegler degree (°SR) of about 90. At least three measurements of °SR were done following standard ISO 5267.

*Phosphorylation of cellulose fibers.* Refined cellulose suspensions at different concentration (1 wt%, 2 wt% or 5 wt% solid content) were mixed with different amount of urea and phosphate salts ($NH_4H_2PO_4$, $(NH_4)_2HPO_4$, $NaH_2PO_4$, $Na_2HPO_4$, $LiH_2PO_4$) for 30 min. The different ratio of AGU/ $HPO_4$/urea used are 1/1.2/4.9, 1/0.32/1.29, 1/1.6/6.58, 1/3.22/12.88, 1/4.83/19.75 and it corresponds to a $(NH_4)_2HPO_4$ concentration of respectively 0.0744, 0.02, 0.1, 0.2, 0.3 mol/L. After that, suspensions at 1 and 2 wt% were filtered until 10 wt% and dried at 105°C according to the protocol of Ghanadpour et al.(Ghanadpour et al., 2015). When the test was made with a cellulose concentration of 5 wt%, fiber suspension was not filtered but directly dried at 105°C. Finally, dried fibers were cured at 150°C for 1h in an oven. After the curing step, fibers were soaked in water at 2 wt%, redispersed and washed several times with boiling water and water under filtration with filter of 1µm.

*Phosphorus content in the filtrate by pH titration.* When cellulose suspension (at 1 or 2 wt%) was filtered until 10 wt% before the drying step, the concentration of phosphate groups in the filtrate was measured. 200 mL of the filtrate was titrated with HCl at 0.5M. The phosphate component reacts with acid to form phosphoric acid.

The concentration of phosphate salt in the filtrate is evaluated and the quantity of phosphate ion adsorbed in mmol per gram of cellulose is then deduced. At least duplicates were performed.

*Total charge content of phosphorylated fibers.* After the curing step and the washing step, the phosphorylated pulp was titrated by conductivity with NaOH. 0.5 g (equivalent dry) of modified cellulose fibers were dispersed in 200 mL of distilled water and the pH was reduced to 3 to convert the hydroxyl groups in their acidic form. The total charge content is measured by titration using NaOH 0.05M. At least triplicates were performed.

*Elemental analysis & ICP analysis.* Carbon, hydrogen, oxygen and phosphorus contents were measured for the different phosphorylated cellulose pulps using a Vario MICRO cube CHNS-O elemental analyzer (Elementar). Phosphorus total content was measured after micro waves mineralization in presence of acid and followed by inductively coupled plasma (ICP). At least two measurements were done for each sample. The degree of substitution was calculated on the basis of the phosphorus content using the following equation:

$$DS = \frac{162 * \%P}{n_{P\ in\ grafted\ mol.} * M(P) - M(grafted\ mol.) * \%P}$$

where %P is the P content determined by ICP, M(P) is the molar mass of phosphore (i.e. 31 g/mol), M(grafted mol.) is the molar mass of the grafted molecule (i.e. 80 g/mol) and $n_{P\ in\ grafted\ mol.}$ is the number of P element in the grafted molecule.

*Degree of polymerization (DP) of cellulose fibers.* DP was evaluated using the ISO 5351:2010 standard. 250 mg (equivalent dry) of phosphorylated cellulose fibers was dissolved in copper (II) ethylenediamine and intrinsic viscosity ($\eta_{int.}$) was measured at least three times. The degree of polymerization (*DP*) was calculated using the Mark-Houwink-Sakurada equation and the intrinsic viscosity as follows:

$$DP^{0.905} = 0.75\ \eta_{int.}$$

At least duplicates were performed.

*Crystallinity Index (CI).* CI of the modified celluloses was obtained using wide-angle X-ray diffraction (XRD) spectra. A PANanalytical X'Pert PRO MPD diffractometer, equipped with

an X'celerator detector was used and X-rays were generated with a copper anode (Kα radiation λ = 1.5419 Å). The cellulose CI (%) was determined according to the peak height method, where $I_{002}$ represents the diffraction intensity of the main crystalline peak at 2θ ≈ 22.5° and $I_{am}$ is the intensity at 2θ ≈ 18.7°. All the samples were tested at least in duplicate.

$$\mathrm{CI} = \frac{(I_{002} - I_{am}) * 100}{\mathrm{I}_{002}}$$

*Optical microscopy images.* Cellulose suspensions were diluted to 0.5 wt% and optical microscopy images were taken. A Carl Zeiss Axio Imager M1 (Germany) optical microscope was used in a transmission mode. A minimum of five pictures were taken for each sample and the most representative is shown here.

*Scanning Electron Microscopy – Energy Dispersive X-ray analysis (SEM-EDX).* Scanning electron microscopy equipped with an energy-dispersive X-ray spectroscopy module (LEO Stereoscan 440). Detector Si (Li) EDAX-10 $mm^2$ was used to evaluate the position of phosphate groups in the fiber. Tension was reduced at 6 keV and the acquisition time was 2h30 in order to increase the resolution.

*X-Ray photoelectron spectroscopy (XPS).* Chemical analysis was also established for the modified and unmodified samples. The test was carried out using a Kα apparatus modulated with a monochromatic Al Kα X-ray source at 14,875 eV. The substrates were positioned at an angle of 90° under an ultrahigh vacuum of less than $10^{-7}$ Pa. Spectrum NT was used to decompose the signal and the overall spectrum was shifted to fix the contribution of C-C in the $C_{1s}$ spectra at 285.0 keV.

The O/C ratio was calculated using the following equation:

$$\frac{O}{C} = \frac{I_O}{S_O} * \frac{S_C}{I_C}$$

where $I_O$ and $I_C$ are the intensity of the oxygen and carbon peaks respectively. $S_C$, $S_O$ and $S_P$ are equal to 0.00170, 0.00477 and 0.0014 for carbon, oxygen and phosphorus respectively. It characterizes the atomic sensitivity factor. P/C ratio was also calculated using this method.

*Nuclear Magnetic Resonance (NMR).* Solid-state NMR experiments were performed on Bruker Avance III HD 11.75 T spectrometer equipped with a 3.2 mm triple resonance low temperature MAS probe and Bruker Avance Neo 21.14 T spectrometer equipped with a 1.3 mm triple resonance MAS probe in double resonance mode. The $^{13}C$ detected $^{1}H$-$^{13}C$ CP, $^{1}H$-

$^{13}C$ HETCOR, 1D $^{1}H$ CRAMPS and 2D $^{1}H$ DQ-CRAMPS experiments for all the samples were carried out on Bruker Avance III HD 11.75 T spectrometer using magic angle spinning (MAS) of 12.5 kHz. The proton detected $^{13}C$-$^{1}H$ HETCOR and $^{1}H$ DQMAS experiments were performed for all the samples on Bruker Avance Neo 21.14 T spectrometer using MAS rate of 62.5 kHz. The proton and carbon spectra were referenced externally by using L-alanine methyl proton as 1.38 ppm and methyl carbon as 20.5 ppm. All the experiments were performed at room temperature.

*Time of Flight-Secondary Ion Mass Spectrometry (ToF-SIMS).* This technique makes possible the molecular structures identification at the top surface of materials (information depth limited to a few monolayers i.e. about 2 to 5nm) and was used here to gain more insight on the grafting mode of the phosphorylation at the surface of the fibers. Measurements were carried out on a TRIFT III ToF-SIMS instrument from Physical Electronics operated with a pulsed 22 keV $Au^{+}$ ion gun rastered over a 300 x 300 $\mu m^2$ area. Data were analyzed using the WinCadence software. Mass calibration was performed on hydrocarbon secondary ions. The relative intensity for a given ion was calculated by dividing the intensity of that ion by the total integrated intensity minus the H intensity which is barely reproducible.

## 3. Results & discussions

### 3.1 Effect of the filtration step on the final charge content of the modified fibers

The objectives of this part are to check if there is adsorption of phosphate ions and to evaluate the influence of the filtration step on the final charge content.

Cellulose fiber suspensions at 1 wt% were mixed with $(NH_4)_2HPO_4$ and urea in quantity described in Methods part and then filtered until 10 wt%. The filtrate was pH titrated in order to measure the non-absorbed phosphate groups and so deduced the charge adsorbed.

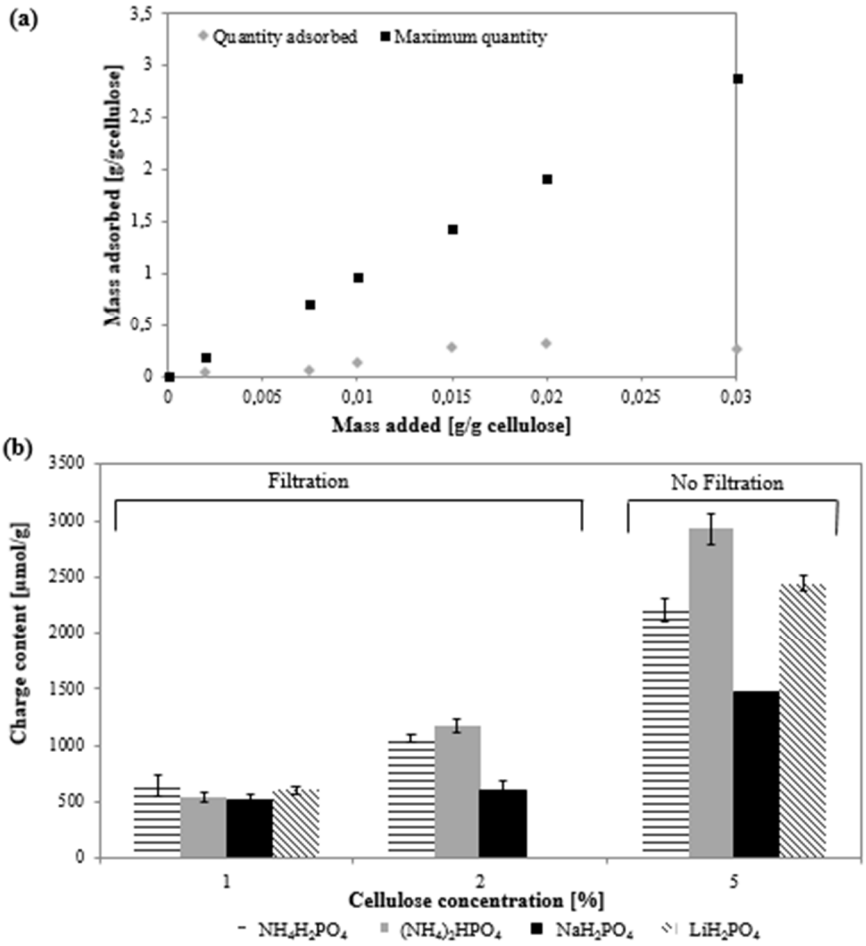


**Figure 1:** Phosphorylation of cellulose fibers (a) adsorption of phosphore depending on mass of phosphate salt added and (b) depending on cellulose concentration and phosphate salt

Salt adsorption increases with the concentration of phosphate salt as shown in Figure 1a. However, the mass adsorbed was very low compared to the mass added. Cellulose fibers which are slightly negatively charged (0.06 mmol/g) due to residual hemicelluloses or cellulose oxidation during bleaching constitute heterogeneous surface and are not favorable to adsorb anionic phosphate salt. Phosphate compound is poorly adsorbed on cellulose fibers and the filtration step before the drying step eliminates most of the salt.

Cellulose concentration and the effect of the filtration step were then studied as reported in Figure 1b. The final charge content increases a lot with the cellulose concentration and was really higher when the filtration step was eliminated whatever the phosphate salts. When cellulose pulp was at 2 wt% solid content, phosphate groups were "closer" to the fibers than at 1 wt% and the adsorption step before the filtration might be improved and so the final charge content. Another explanation is the fibers entanglement. At 2 wt% entanglement was increased and phosphate salts were trapped easily in the fibrous mat during the filtration. Both options result in higher modification rate.

When phosphorylation occurs, fiber swells and may even be dissolved as reported by Ghanadpour et al.(Ghanadpour et al., 2015) and confirmed by optical microscopy in Figure S4. We supposed that phosphorylation starts at the fiber surface and then thanks to the swelling, phosphate salts can reach the core of the fibers. When phosphate ion was just adsorbed on the surface, charge content was lower. On the contrary, when filtration step was eliminated, excess of phosphorus was present and the phosphorylation can go further from the surface to the core. This fact is confirmed by Noguchi et al.(Noguchi et al., 2017) who obtained higher charge content using high cellulose concentrated medium and lower phosphate salt concentration (ratio 1/0.63/3.22 compared to a ratio of 1/1.2/ 4.9 with filtration). Eliminating the filtration step constitutes a good option to increase the charge content without increasing the chemicals consumption.

### 3.2 Urea role during the phosphorylation of cellulose fibers

Urea has already been used in many protocols to prevent the degradation of cellulose (Ghanadpour et al., 2015; Noguchi et al., 2017; Nuessle et al., 1956; Suflet et al., 2006), to act as a catalyst (Lagier, Zuriaga, Monti, & Olivieri, 1996; Yurkshtovich, Yurkshtovich, Kaputskii, Golub, & Kosterova, 2007) or to enhance the fibers swelling and hence increase the phosphate groups penetration. Urea effect was investigated as reported in Table 1.

**Table 1:** Influence of urea content in cellulose phosphorylation

| Cellulose concentration | Molar ratio AGU/ $(NH_4)_2HPO_4$ / Urea | Charge content [mmol/g] | Cellulose color | Presence of aggregate |
|---|---|---|---|---|
| 2 | 1/0/0 | 0.06 ± 0.01 | White | No |
| 2 | 1/0/4.9 | 0.17 ± 0.03 | White | No |
| 2 | 1/1.2/0 | 0.37 ± 0.01 | Black | Yes |
| 2 | 1/1.2/4.9 | 1.18 ± 0.06 | Brown | Yes |
| 2 | 1/1.2/7.2 | 2.37 ± 0.05 | Yellow | Yes |

Without urea, the phosphorylation only slightly occurs with a charge content of 0.37 mmol/g whereas the cellulose became totally black. It is now clear that urea is necessary to phosphorylated cellulose but also to prevent cellulose degradation. One reactional mechanism adapted from Kokol et al.(Kokol, Božič, Vogrinčič, & Mathew, 2015) is presented in Figure 2 with several phosphorylated cellulose structure possibilities. Urea has an active role in the reaction but also in the protection of the cellulose. Presence of nitrogen basic elements in the phosphorylation process seems primordial (Katsuura & Mizuno, 1966; Nuessle et al., 1956; Reid & Mazzeno, 1949; Reid et al., 1949).

When urea content increased, charge content increased and the coloration of cellulose decreased. Yurkshtovich et al.(Yurkshtovich et al., 2007) showed that phosphorus content increased with the concentration of urea up to 3.33M (i.e. 4 times higher than what we used here). However side reaction can occur and creates carbamate. This is not a problem from a nanofibrillation point of view, because it also weakens the H-bonds between cellulose nanofibrils.

### 3.3 Influence of phosphate salt solubility and pH on the final charge content

Up to our knowledge, no study dedicated to phosphorylated CNF has compared various phosphate salts. In this study, higher modification rates were expected with an higher constant of solubility (Ks). Unfortunately, no relationship between the degree of substitution and the Ks was observed even if various phosphorylation rates are clearly obtained, depending on the phosphate salt Ks as reported on Table 2. However, if the Ks is very low (for example $Na_2HPO_4$), the grafting was very low. Indeed, the counterion was closer due to lower dissociation and there was some hindrance and less reactivity.

For a same counterion, the total charge content increased if the Ks increased, meaning that counterion have more impact than Ks. In each case, the counterion ammonium ($NH_4^+$) led to

higher DS than lithium ($Li^+$) and than sodium ($Na^+$). For now, counterion effect in the chemical reaction is still under discussion (Manet, 2007). Some studies reported that in concentrated sodium hydroxide media, $NH_4^+$ have a lower affinity with hydroxyl groups and will not surround the anhydroglucose units. Moreover, the ammonium counterion has a lower affinity for water than sodium ion. The more hydrophobic character of $NH_4^+$ would produce more pronounced swelling of the cellulose as the non-activated anhydroglucose unit will be repelled (Ott, Spurlin, Grafflin, Bikales, & Segal, 1954). In water, lithium ion is more hydrated than sodium followed by ammonium. Counterion electronegativity can also influence the reaction. Lithium and sodium with an electronegativity of respectively 0.98 and 0.93 are much less electronegative than nitrogen (3.04) and so the quaternary ammonium. The distance between $NH_4^+$ and $HPO_4^{2-}$ is longer than the one between $Li^+$ or $Na^+$ and $HPO_4^{2-}$ due to lower difference of electronegativity. $NH_4^+$ is more distant of $HPO_4^{2-}$ than the other counterion and so salts are less stable (or more reactive) which leads to higher grafting.

**Table 2:** Influence of phosphate salt constant of solubility (Ks) and pH, on cellulose phosphorylation using AGU/Phosphate salt/ urea ratio of 1/1.2/4.9 and cellulose fiber concentration of 5 wt% without filtration. *pH was modified by adding NaOH or HCl

| Phosphate salt | Ks | Cellulose concentration [%] | pH | Charge content [mmol/g] | Equivalent DS | DS based on P content [AE] |
|---|---|---|---|---|---|---|
| $LiH_2PO_4$ | 126 | 5 | 9* | 2.15 ± 0.31 | 0.35 | - |
| $LiH_2PO_4$ | 126 | 5 | 5 | 2.44 ± 0.07 | 0.39 | 0.18 |
| $NaH_2PO_4$ | 94.9 | 5 | 10* | 0.48 ± 0 .12 | 0.08 | - |
| $NaH_2PO_4$ | 94.9 | 5 | 4 | 1.48 ± 0.12 | 0.24 | 0.29 |
| $(NH_4)_2HPO_4$ | 68.9 | 5 | 8 | 2.93 ± 0.14 | 0.47 | 0.45 |
| $(NH_4)_2HPO_4$ | 68.9 | 5 | 4* | 4.40 ± 0.50 | 0.71 | - |
| $NH_4H_2PO_4$ | 37.4 | 5 | 4 | 2.21 ± 0.10 | 0.36 | - |
| $Na_2HPO4$ | 12 | 5 | 8 | 0.41 ±0.01 | 0.07 | - |

The pH effect was also investigated. For every phosphate salt, the reactivity and the final charge content was higher when acidic medium was used as confirmed by Lim and Seib on wheat starch (Lim & Seib, 1993). For example, charge content passes from 0.5 to 1.48 mmol/g for $NaH_2PO_4$ or from 2.93 to 4.40 for $(NH_4)_2HPO_4$. Indeed at acidic pH, two OH groups are available on the phosphate salt and the reaction is improved. Moreover, in acidic medium, negative charges of cellulose are reduced and anionic phosphates are not repelled.

### 3.4 Chemical structure of the grafted cellulose fibers

As shown in the Figure 2, different cellulose structures can be obtained after the phosphorylation. Hydroxyl groups of cellulose can react with phosphate salt and form phosphate groups (Cell-O-P(O)$(OH)_2$), phosphite groups (Cell-O-P$(OH)_2$) or combination. Crosslinking can also occur (Noguchi et al., 2017). Some aggregates are formed during the curing step and are really difficult to destroy and might correspond to crosslinked structures. Moreover, position of phosphate groups on the cellulose units and its penetration on the fiber is not so evident. Different methods were investigated to determine which form is the preferential one and how fibers are modified.

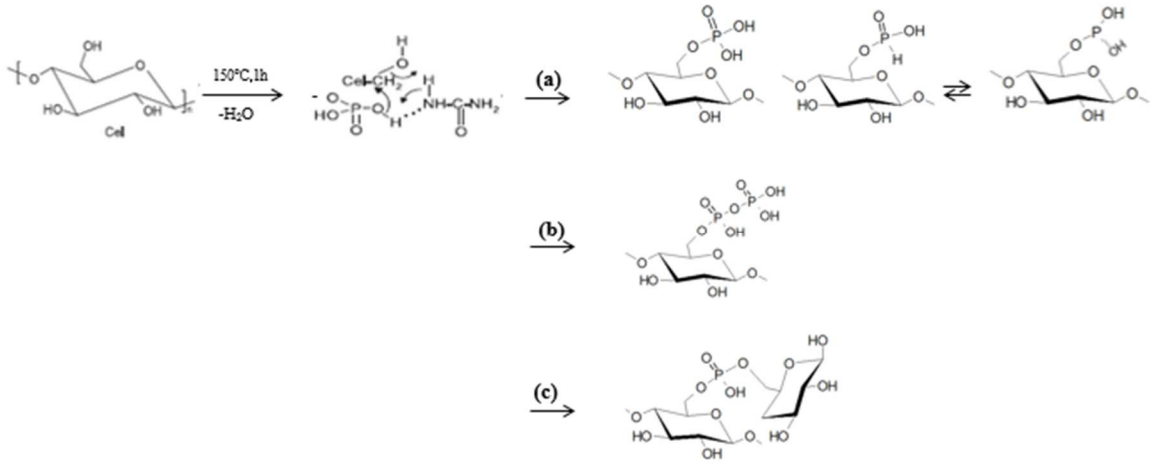


**Figure 2:** Different grafting modes for phosphorylated cellulose as proposed by Kokol et al.(Kokol et al., 2015)

#### 3.4.1 Conductivity titration

The first method that might give information about the cellulose structure is the conductimetric titration (Figure S1). The degree of substitution measured by elemental analysis is equal to the one obtained by conductimetric titration as reported in Table 2 and confirmed by Naderi et al.(Naderi et al., 2016). During the titration only one pH jump is observed meaning that only one hydroxyl group is titrated. This can suppose that the phosphate group form is the one in Figure 2a, (second form) or that there is crosslinking like in scheme Figure 2c. However Kokol et al.(Kokol et al., 2015) reported pKa of 6.8 and 12.5 for (Cell-O-$PO_3H_2$/ Cell-O-$PO_3H^-$) and cell-$CH_2$-O-$PO_3^{2-}$. Most of the time the titration was done between pH 2 and 11 meaning that the second hydroxyl groups of the phosphate group is not measured which means that all the form presented in Figure 2 could be obtained.

However, even when the pH was increased until 13 for some trials, only one pH jump was reported.

### 3.4.2 Solid-State NMR

*High-resolution solid-state NMR at 11.74 Tesla*

Native and phosphorylated cellulose fibers were analyzed at 11.74 T (500 MHz for $^{1}H$ resonance) using $^{13}C$, $^{31}P$ and $^{1}H$ NMR analyses as reported in Figures 3 and 4 to determine where the phosphorus is located. The $^{13}C$ NMR spectrum is shown in Figure 3a. The respective spectra of cellulose and phosphorylated cellulose are consistent with the data reported in the literature. The peak in the 58-68 ppm region corresponds to the C6 of the cellulose ring, in 68-80 ppm region to C2, C3 and C5 carbon, from 80 to 91 ppm to the C4 and finally from 101 to 109 ppm to the C1 (Atalla & Vanderhart, 1984). Note that signals at 84 ppm and 63 ppm are respectively assigned to C4 and C6 of amorphous domains of celluloses (Atalla & VanderHart, 1999; Montanari, Roumani, Heux, & Vignon, 2005). As their spectra appear to be very alike, it indicates that the carbon structure of the phosphorylated cellulose fibers with a charge content of 2.10 mmol/g might be not significantly modified compared to the carbon structure of the pristine cellulose. Ghanadpour et al.(Ghanadpour et al., 2015) also reported that all the regions of modified fibers are slightly changed and thus no region selectivity is observed. In our case, it could indicate that the phosphate grafting was homogenously distributed on the cellulose fibers which do not lead to specific changes in the $^{13}C$ chemical shift.

The presence of phosphorus on the cellulose fibers after a strong washing step is confirmed by an intense signal in the HPDEC $^{31}P$ NMR spectra as shown in Figure 3b. The phosphorus components appeared in the region -10 to 10 ppm it is mainly made of an intense signal at 0 ppm overlapping a broader low intensity signal which spreads down -15 ppm.

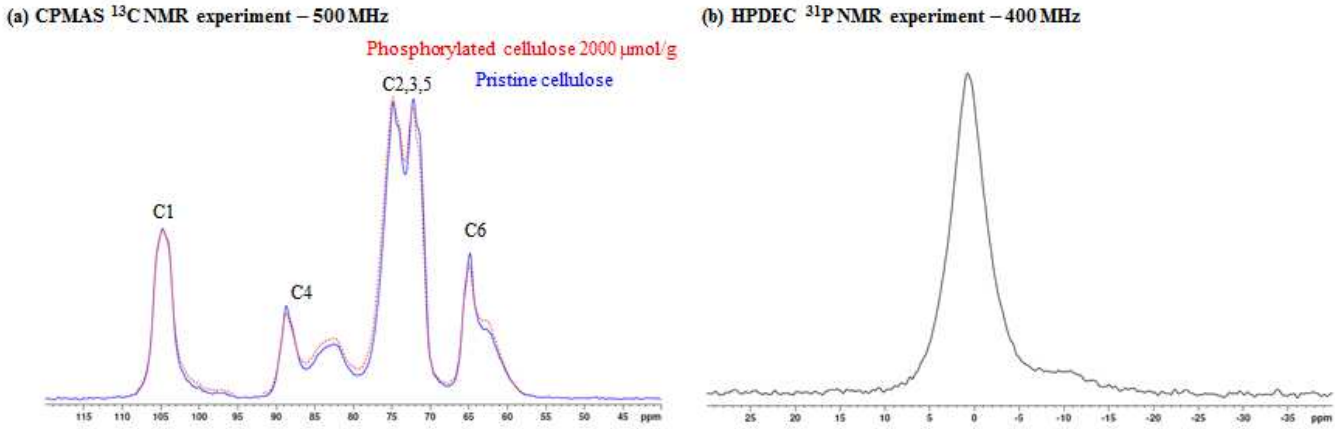


**Figure 3:** Influence of the phosphorylation on the carbon structure of the cellulose: (a) $^{13}C$ solid-NMR spectra and (b) HPDEC $^{31}P$

At a 11.7 T field high-resolution solid-state $^{1}H$ NMR spectra of both pristine and phosphorylated cellulose were obtained with DUMBO sequence and reported in Figure 4a. Very interestingly, contrarily to their carbons counterparts the proton spectra present some significant differences. We can observe a low shift of the maximum intensity from pristine to grafted celluloses. Moreover, the spectra of the grafted cellulose present two large and intense shoulders between 5 and 7 ppm. Similar signals are also observed in the pristine cellulose but much less intense. It means that new type of protons appeared during the phosphorylation. Those new protons can be due to either (i) hydroxyl protons at the phosphate groups grafted on cellulose or (ii) modifications of the hydrogen bond network. This latter statement can be supported by the number of oxygens, brought by the phosphorylation, that are good candidate to modify the hydrogen bond network. As protons resonances are shifted to the high frequencies we can infer that the amount of proton involved in hydrogen bond network is increased.

To have more information concerning the proton network of the phosphorylated and pristine celluloses, dipolar proton-carbon correlation experiments were carried out and reported in Figure 4b.

The 2D maps (normalized related to the intensity of signals of crystalline C4) look very similar, however some differences can be noticed. In Figure 4b, showing the dipolar interactions between C and H, the proton resonances of the phosphorylated cellulose are shifted to the higher frequency except the protons in interaction with C4 of crystalline

domains. Due to the normalization, it appears that the amount of C4 in amorphous domain is increased (larger correlation). In a similar way the correlation assigned to C2,3,5 appears to be broader in the phosphorylated cellulose that in the pristine one. The correlation at C1 is not significantly affected.

On the base of the expected chemistry of phosphorylation, grafting should occur mainly at C6. Therefore the broadening that we mentioned previously of C2,3,5 correlations at around 68 ppm could be assigned not to chemical shift changes of theses carbons but mainly to the effect of substitution on C6 which leads to a low field effect and consequently to the observed signal broadening of C2,C3,C5 correlation. Moreover grafting mainly appears on amorphous domain (increase of the amorphous C4).

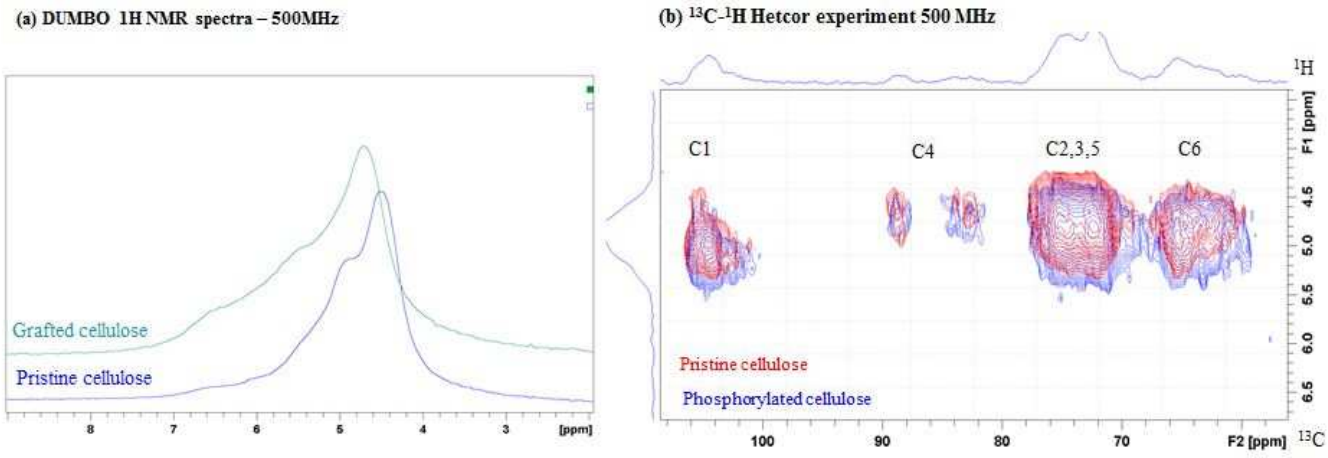


**Figure 4:** Solid-NMR spectra. Effect of the phosphorylation on the proton network of cellulose fibers. (a) Hetcor experiment and (b) DUMBO experiment

*High-resolution solid-state NMR at 21.1 Tesla*

The spectra recorded at 21.1 T with MAS rate of 62.5 KHz bring some complementary information. On an experimental point of view, to the fact that very high spinning rates are used, some consequences are expected. For $^{1}H$ NMR, spectra can be acquired either with direct excitation or with spin echo experiment. For the dipolar $^{1}H$-$^{13}C$ correlation experiments (proton detected at this field), it has to be mentioned that due to the high spinning rate of the samples the molecular domains with small proton carbon dipolar interactions can be difficult to detect. In that case the experiment enhances the crystalline parts of pristine or phosphorylated celluloses. Taking into account these observations the following conclusions can be drawn.

The $^{1}H$ NMR recorded at 21.1 T and shown in Figure 5,a confirms the results obtained at 11.7 T, namely the presence of new signals at 5 and 7 ppm. Note that for the pristine cellulose the signal at 4.2 ppm is assigned to water molecules which can be identified by adding small quantity of water to the sample and which are very sensitive to the temperature.

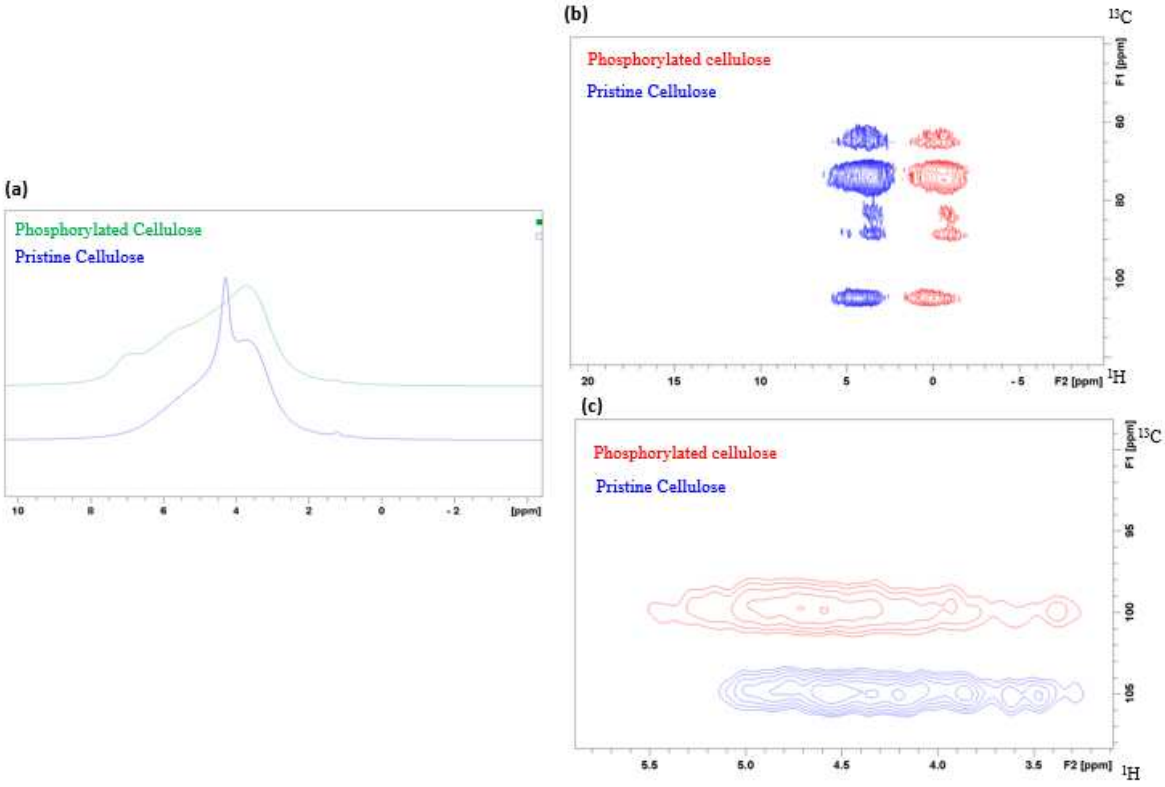


**Figure 5:** (a)$^{1}H$ NMR recorded at 21.1T for pristine cellulose and phosphorylated cellulose; (b) and (c) Proton-carbon correlation recorded at 21.1 T. Influence of the phosphorylation on the cellulose structure

Contrary to the 2D $^{1}H$-$^{13}C$ correlation experiments recorded at 11.7 T the 2D spectra recorded at 21.1 T are very similar, as shown in Figure 5b,c . It has to be reminding that in that case we mainly see the crystalline domain of the materials. However the C1 are correlated to protons that appear to be slightly shifted at higher frequency in the phosphorylated cellulose compared to pristine.

At such field, due to the fast spinning rate and the low amount of material that are analyzed in the order of a few mgs, direct detection of $^{13}C$ NMR is impossible within reasonable experiment time. The only way to obtain an equivalent 1D spectrum is to calculate the sum of the columns (carbon in the indirect dimension). The calculated spectra are shown in Figure 6 and contrary to the $^{13}C$ spectrum acquired at 11.7 T the spectra present some differences. The

feature of the calculated spectrum of phosphorylated cellulose appears to be more crystalline than the pristine one. It is a strong indication that the phosphorylation of cellulose fibers lead to amorphous domains which are not seen in the 2D experiments recorded under these conditions, i.e., 21.1 T and 62500 Hz of spinning rate.

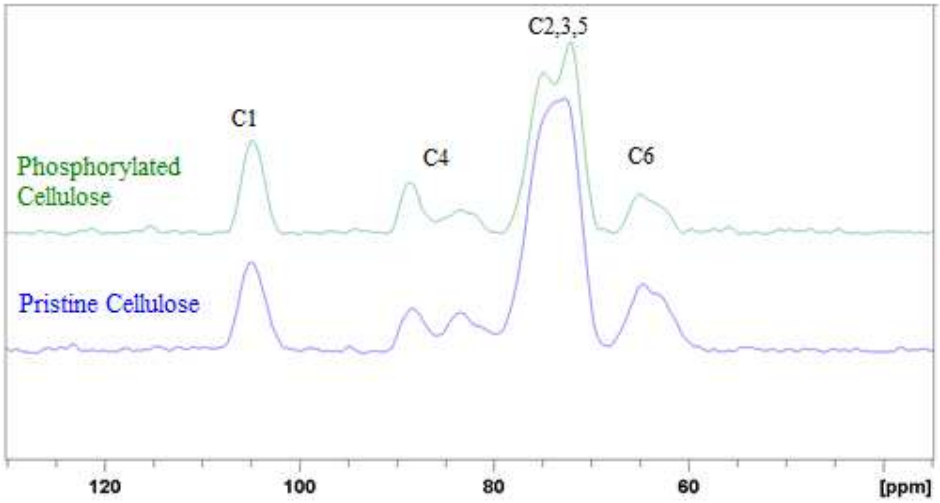


**Figure 6:** Reconstituted $^{13}C$ NMR 1D spectrum of pristine cellulose and phosphorylated cellulose

To conclude, the NMR analysis cannot help to determine which exact structure of the phosphorylated cellulose fiber is formed insofar as the carbon structure is not affected and the proton network is entirely modified. However, the phosphorylation is clearly visible regarding the $^{31}P$ spectrum or with the change in the proton network.

### 3.4.3 Time of Flight-Secondary Ion Mass Spectrometry

ToF-SIMS analyses were performed at the surface the phosphorylated cellulose fibers to try to determine the preferential grafting mode of phosphorylation at the extreme surface of cellulose fibers. Results are displayed in Figures 7 and S2 and relative intensities of specific signatures are given in Figure S3.

The phosphate salt, $(NH_4)_2HPO_4$, used for the phosphorylation of cellulose was analyzed in its original form and several characteristics peaks were found: in the negative mode, $PO_2^-$ (m/z = 62.96), $PO_3^-$ (m/z = 78.96) and $H_2PO_4^-$ (m/z = 96.97) which are the typical peaks detected for phosphorylated compounds but also $HP_2O_6^-$ (m/z = 158.93), $H_3P_2O_7^-$ (m/z = 176.93) and $H_5P_2O_8^-$ (m/z = 194.95) and in the positive mode, $NH_3H_3PO_4^+$ (m/z = 116.01).

The peaks at m/z = 120.96 and 142.95 in the positive mode correspond to $NaH_3PO_4^+$ and $Na_2H_2PO_4^+$, respectively, and indicate a cationization effect related to Na (a significant intensity is also detected for $Na^+$). The detection of $HP_2O_6^-$ (m/z = 158.93), $H_3P_2O_7^-$ (m/z = 176.93) and $H_5P_2O_8^-$ (m/z = 194.95) indicates a dimer alike based emission.

In the spectra of phosphorylated fibers, there was no detection of high mass molecular peaks combining cellulose and the grafted moieties. On the other hand, no new phosphorus-based secondary ions were detected.

In the positive mode spectra of phosphorylated fibers, the peak at m/z = 116.01 corresponding to $NH_3H_3PO_4^+$ was not detected, which can confirm the grafting as well as an efficient washing step. Furthermore, urea displays a characteristic peak around at m/z = 61.03, as shown in Figure S2, and this peak is not detected on the phosphorylated fibers meaning that the washing step was efficient.

The spectra of phosphorylated fibers in the negative mode show some signatures of the reference powder. $PO_2^-$ (m/z = 62.96), $PO_3^-$ (m/z = 78.96) and $H_2PO_4^-$ (m/z = 96.97) are detected in the modified cellulose fibers but their relative intensities are different for the various samples (see Figure 7 and S3). Hence, a detailed study of the relative intensity of the above described secondary ions was undertaken.

The relative intensities of $PO_2$, $PO_3$ and $H_2PO_4$ are similar for the phosphorylated pulps with charge contents of 2.93 and 1.18 mmol/g (taking into account standard deviations) but they are significantly different for the charge content equal to 0.54 mmol/g. This indicates a different extent in the way of grafting, observed as a function of the different quantity of phosphate salt added in the suspension. On the other hand, intensities are also different in the spectra of the modified celluloses and in the spectra of the reference powder, which could then help understanding what is the probable referred grafting mode among those displayed in Figure 2. One must still be careful as no reference sample of the proposed grafting modes could be available for ToF-SIMS analysis.

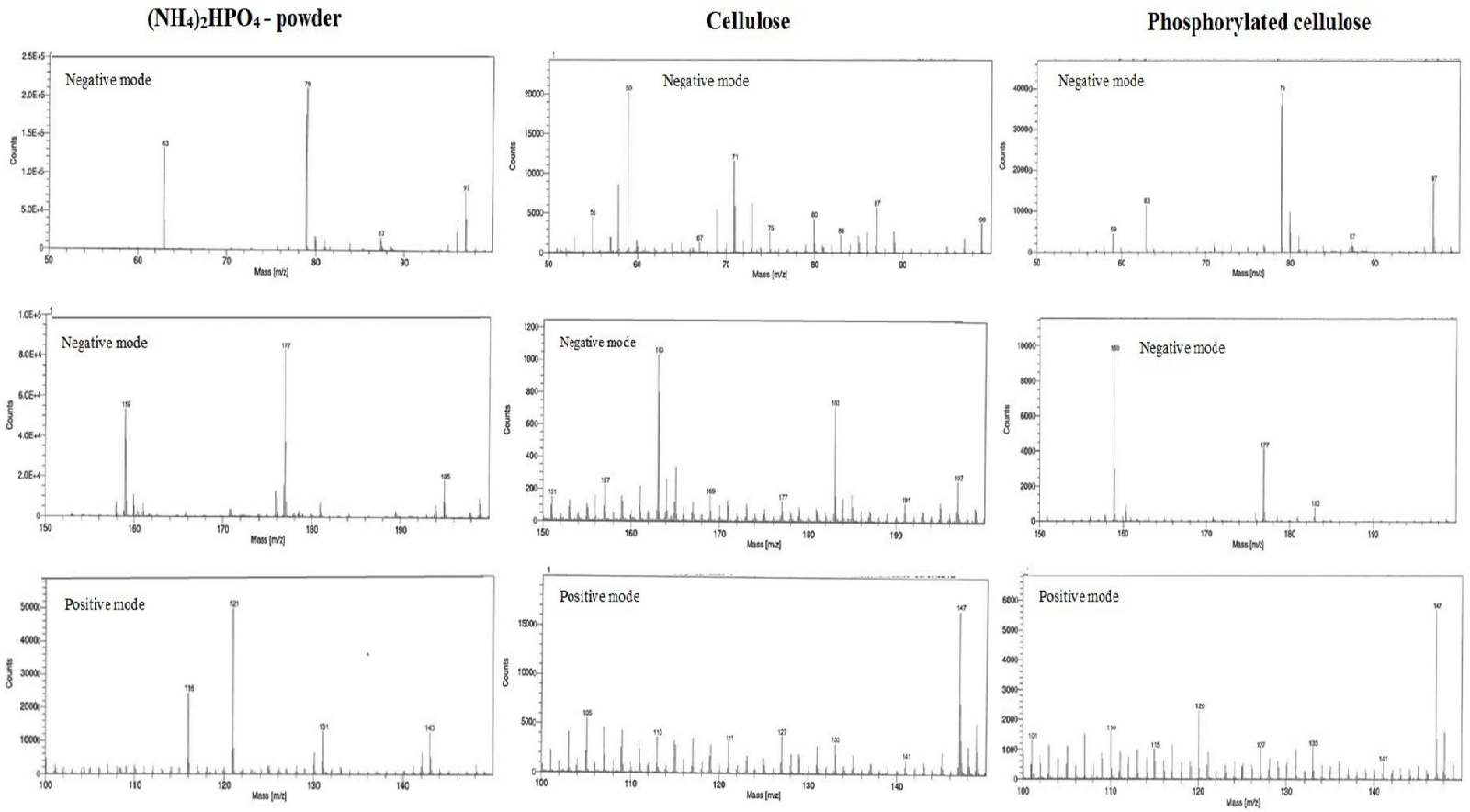
(NH4)2HPO4 - powder
Cellulose
Phosphorylated cellulose
Negative mode
Positive mode
Counts
Mass [m/z]

**Figure 7:** ToF-SIMS spectra of phosphate salt powder, pristine cellulose and phosphorylated cellulose fibers in the positive in the 100-150 m/z range and in the negative modes in the 50-100 and 150-200 m/z range

$PO_3^-$ (m/z = 78.96) and $H_2PO_4^-$ (m/z = 96.97) are the most preponderant secondary ions for the modified fibers and their normalized intensity (according to $PO_2$ intensity) decreased when grafting rate decreases. This can confirm that most of the phosphorylated fibers are in the form of Figure 2a.

Moreover, the peaks at $HP_2O_6^-$ (m/z = 158.93), $H_3P_2O_7^-$ (m/z = 176.93) are detected in the phosphorylated cellulose fibers (the peak at m/z = 194.95 m/z exhibits a very low relative intensity) but their relative intensities are really different, even between the samples with charge contents of 2.93 and 1.18 mmol/g. The presence of this species increases with the charge content from 0.54 to 2.93 mmol/g whereas the intensities of $PO_2$, $PO_3$ and $H_2PO_4$ increase for a charge content from 0.5 to 1.1 and then tend to stabilize.

Those species can be present due (i) to the grafting of the impurities of the phosphate salt powder on the fibers, (ii) due to the grafting of two $HPO_4^{2-}$ ions on the cellulose, (iii) due to the grafting of this species present in the powder on the cellulose fibers or due to (iv) possible recombination during the analysis.

Their intensities in the functionalized fibers are different and this can be explained by different reasons. First, if $HPO_4^{2-}$ is grafted on the fibers, the combinations are less possible and those species cannot be formed. $HPO_4^{2-}$ is not free and cannot make combination. However, in this case, if all the $HPO_4^{2-}$ were grafted, the peaks at 158.93 and 176.93 m/z would have totally disappeared. The presence of these two peaks at 158.93 and 176.93 m/z can also relate the grafting of those species present in the powder or the combination of two $HPO_4^{2-}$ and formation of di or tri ester as reported in Figure 2b. The formation of the cellulose structure described in Figure 2c should lead to new peaks and none are visible.

To conclude, no characteristic peak of the phosphorylated cellulose has been clearly identified by ToF-SIMS analysis but some hypothesis of grafting was determined. It seems that the phosphorus is present on the cellulose fiber with the $H_2PO_4^-$ form and in a fewer extent $HP_2O_6$. The presence of crosslinked cellulose structures has been discarded insofar as no signal was detected. This technique analyzes the extreme surface whereas some phosphate

485 salt can penetrate. That is why an intermediate surface technique (XPS) was performed to
486 carry on investigations.

487 **3.4.4 X-ray photoelectron spectroscopy**

488 The phosphorylated pulp with a charge content of 2.10 mmol/g and the pristine cellulose
489 were analyzed as reported in Figure S4. Total spectra of native and phosphorylated cellulose
490 are presented in Figure S4a. Distinct peaks of $C_{1s}$ and $O_{1s}$ are present on the native cellulose
491 as well as minor peaks characteristics of surface contamination. Additional peaks are present
492 on the phosphorylated cellulose. The peaks characteristics of the phosphorus appeared at
493 134.4 eV and 190.5 eV and are assigned to $P_{2p}$ and $P_{2s}$ (Božič, Liu, Mathew, & Kokol, 2014;
494 Ghanadpour et al., 2015; Pasqui, Rossi, Di Cintio, & Barbucci, 2007), confirming the
495 phosphorylation. The peak at 401.4 eV corresponds to the presence of nitrogen (Bourbigot, Le
496 Bras, Gengembre, & Delobel, 1994) $N_{1s}$ which is probably assigned to $NH_4^+$ groups of the
497 phosphate salt.

498 The scan spectra of $C_{1s}$ of the native cellulose and the phosphorylated cellulose are
499 presented in Figure S4c and d. The spectra are decomposed in 4 peaks characteristics of the
500 cellulose, namely, C1(C-C), C2 (C-O), C3 (C=O) and C4 (O-C-O) at respectively, 285.0,
501 286.6, 287.8, 289.2 eV. The two spectra present high differences especially regarding the C1
502 and C2 peaks. Indeed, the grafting of phosphate groups can change the chemical environment
503 of the carbon and thus increases the C-C peak while decreasing the C-O peak (Božič et al.,
504 2014). The intensity of C-C peak increases and this can be due to the presence of phosphate
505 groups covering all of the outer surface of fibers (Ghanadpour et al., 2015; Li, Wang, Liu,
506 Xiong, & Liu, 2012).

507 The relative surface concentration of C, O and P atoms were calculated by integrating the
508 peaks of each element and results are presented in Table S1. Unfortunately after
509 phosphorylation the O/C ratio does not increase whereas a lot of oxygen is supposed to be
510 added on the cellulose with the phosphorus grafting. Indeed, one free hydroxyl groups of the
511 pristine cellulose is substituted by two new hydroxyl groups and one phosphoryl group (Božič
512 et al., 2014; Granja et al., 2001).

513 Regarding the $O_{1s}$ scan of phosphorylated cellulose, in Figure S4f, a very small asymmetry
514 is detected and the peak can be decomposed in two peaks: 532.7 eV for O1(C-O) and 531.5
515 eV for O2 (P-O) which confirms once again the phosphorylation (Bourbigot et al., 1994). The

DS of the phosphate groups on the cellulose fibers is estimated as follow according to Li et al.(Li et al., 2012). The obtained value is reported in Table S1.

$$DS = \frac{O2}{O1 + O2}$$

The tested phosphorylated pulp presents a charge content of 2.10 mmol/g which corresponds to a DS of 0.32. Here, the obtained DS is three times lower as reported in Table S1. Indeed, XPS measured the surface grafting whereas the titration measure the bulk grafting. The difference can be explained by different points: (i) some phosphorus can be embedded in the fibers network and unseen by XPS, however, we considered that fibers are well washed, (ii) the fibers washing is more efficient in surface than in the inner structure of the cellulose which results in lower grafting, (iii) the grafting is heterogeneous and the analysis was done on a poorly grafted part of the fibers surface.

To conclude, phosphorus was detected by XPS analysis but no information on the phosphorylated cellulose structure is obtained using this technique.

### 3.4.5 SEM EDX

The phosphate group position on the fiber was then evaluated using SEM-EDX on a sectional view of phosphorylated cellulose paper with a charge content of 2.1 mmol/g as reported in Figure 8. Phosphorus is present in huge quantity and covered entirely the sample. Even if the image scale is important compared to the fiber diameters some fibers are visible in sectional view and framed in red. It seems that phosphate groups penetrate the fiber diameter and are homogeneously distributed.

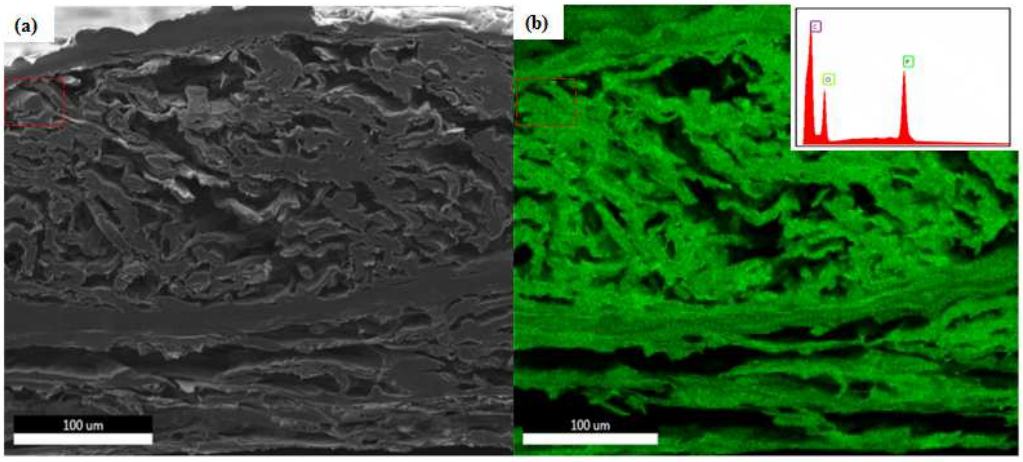


**Figure 8:** Evaluation of phosphorus position on the cellulose fibers (2.93 mmol/g) using EDX images with (a) MEB images and (b) coloration of phosphorus group in green

## 3.5 Influence of the phosphorylation step on cellulose fibers

Fiber degradation traditionally occurs during cellulose chemical pretreatment. Cellulose degradation due to the phosphorylation is evaluated measuring the degree of polymerization and the crystallinity index as reported in Figure S5.

Partial swelling of fibers was observed when the charge content increased as well as a small decrease in the crystallinity index (CI). Cellulose phosphorylation induces a fiber swelling which can lead to some dissolution. A ballooning effect is visible for the sample containing 2.9 mmol/g of phosphate group but fibers morphologies are still maintained.

However, despite the high charge content of 2.9 mmol/g, cellulose I form was maintained and suitable CI was obtained. Noguchi et al.(Noguchi et al., 2017) reported no crystallinity change when the charge content varied from 0 to 2.2 mmol/g. Increasing the charge content will drastically improve the nanofibrillation step without affecting too much the cellulose fibers structure and morphology. This is confirmed by the absence of modification of the carbon spectra in NMR analysis.

The degree of polymerization (DP) of the phosphorylated cellulose pulp with a charge content of 2.1 mmol/g was measured. The phosphorylated pulp presents a DP of 628 ± 5 whereas the refined cellulose pulp presents a DP of 1,200. Phosphorylation as other chemical pretreatments used to weaken cellulose fibers, decreases the DP of the fibers. Rol at al.(Rol et al., 2017) reported a DP decrease of 50 and 75% for respectively enzymatic pretreatment and TEMPO-oxidation of cellulose fiber. As observed in Figure S5 phosphorylation can lead to fiber partial swelling which can result in some dissolution and thus induce a DP decrease. Plus, during the phosphorylation, acid can be released and lead to DP decrease.

To conclude, phosphorylation leads to some fiber DP decreases and can lead to some fibers swelling which will further help the nanofibrillation but preserves the cellulose crystalline structure.

## 4 Conclusion

The phosphorylation of cellulose fibers was studied and optimized to increase the final charge content. Different phosphate salts were tested and no effect of the Ks was reported whereas the presence of ammonium counterion improves the modification rate. A poor adsorption of phosphate ions on the cellulose fibers was reported and the filtration step should be eliminated to strongly increase the charge content. However, the grafting should be limited to avoid fiber dissolution. The grafted molecule position in the cellulose fibers and the chemical structure of the phosphorylated fibers were investigated using several high level

techniques such as NMR, XPS, ToF-SIMS or SEM EDX. NMR analysis confirms that the phosphorylation impacted all the protons network of the cellulose and that the reaction mainly occurs in amorphous area of the cellulose fibers. Finally, it seems that phosphate groups do not affect significantly the physical properties of cellulose fibers.

**Acknowledgment**

This research was supported by Institut Carnot Polynat (Grant agreement n° ANR-16-CARN-0025-01), Centre Technique du Papier (Grenoble, France) and LabEx Tec 21 (Grant agreement n° ANR-11-LABX-0030). LGP2 is part of the LabEx Tec 21 (Investissements d'Avenir) and Institut Carnot Polynat.

## References

Aoki, D., & Nishio, Y. (2010). Phosphorylated cellulose propionate derivatives as thermoplastic flame resistant/retardant materials: influence of regioselective phosphorylation on their thermal degradation behaviour. *Cellulose*, *17*(5), 963–976. https://doi.org/10.1007/s10570-010-9440-8

Atalla, R. H., & Vanderhart, D. L. (1984). Native cellulose: a composite of two distinct crystalline forms. *Science (New York, N.Y.)*, *223*(4633), 283–285. https://doi.org/10.1126/science.223.4633.283

Atalla, R. H., & VanderHart, D. L. (1999). The role of solid state 13C NMR spectroscopy in studies of the nature of native celluloses. *Solid State Nuclear Magnetic Resonance*, *15*(1), 1–19. https://doi.org/10.1016/S0926-2040(99)00042-9

Bardet, R., Bras, J., Belgacem, N., Agut, P., & Dumas, J. (2014). *Patent No. WO 2014118466 (A1)*.

Bourbigot, S., Le Bras, M., Gengembre, L., & Delobel, R. (1994). XPS study of an intumescent coating application to the ammonium polyphosphate/pentaerythritol fire-retardant system. *Applied Surface Science*, *81*(3), 299–307. https://doi.org/10.1016/0169-4332(94)90287-9

Božič, M., Liu, P., Mathew, A. P., & Kokol, V. (2014). Enzymatic phosphorylation of cellulose nanofibers to new highly-ions adsorbing, flame-retardant and hydroxyapatite-growth induced natural nanoparticles. *Cellulose*, *21*(4), 2713–2726. https://doi.org/10.1007/s10570-014-0281-8

Brodin, F. W., Gregersen, O. W. & Syverud, K. (2014). Cellulose nanofibrils: Challenges and possibilities as a paper additive or coating material: A review. *Nordic Pulp and Paper Research Journal*, *29*(01), 156–166. https://doi.org/10.3183/NPPRJ-2014-29-01-p156-166

Chaker, A., & Boufi, S. (2015). Cationic nanofibrillar cellulose with high antibacterial properties. *Carbohydrate Polymers*, *131*, 224–232. https://doi.org/10.1016/j.carbpol.2015.06.003

Coleman, R. J., Lawrie, G., Lambert, L. K., Whittaker, M., Jack, K. S., & Grøndahl, L. (2011). Phosphorylation of alginate: synthesis, characterization, and evaluation of in vitro mineralization capacity. *Biomacromolecules*, *12*(4), 889–897. https://doi.org/10.1021/bm1011773

Davis, F. V., Findlay, J., & Rogers, E. (1949). 52—the Urea-Phosphoric Acid Method of Flameproofing Textiles. *Journal of the Textile Institute Transactions*, *40*(12), T839–T854. https://doi.org/10.1080/19447024908660067

Dufresne, A. (2013). Nanocellulose: a new ageless bionanomaterial. *Materials Today*, *16*(6), 220–227. https://doi.org/10.1016/j.mattod.2013.06.004

Gallagher, D. M. (1965). *Phosphorylation of cotton with inorganic phosphates*. Retrieved from https://patents.google.com/patent/US3488140A/en

Ghanadpour, M., Carosio, F., Larsson, P. T., & Wågberg, L. (2015). Phosphorylated Cellulose Nanofibrils: A Renewable Nanomaterial for the Preparation of Intrinsically Flame-Retardant Materials. *Biomacromolecules*, *16*(10), 3399–3410. https://doi.org/10.1021/acs.biomac.5b01117

Granja, P. L., Pouységu, L., Pétraud, M., De Jéso, B., Baquey, C., & Barbosa, M. A. (2001). Cellulose phosphates as biomaterials. I. Synthesis and characterization of highly phosphorylated cellulose gels. *Journal of Applied Polymer Science*, *82*(13), 3341–3353. https://doi.org/10.1002/app.2193

Ichikawa, S., Wada, S., Masuda, S., & Hasegawa, T. (1979). *Patent No. JP54138060A*.

Inagaki, N., Nakamura, S., Asai, H., & Katsuura, K. (1976). Phosphorylation of cellulose with phosphorous acid and thermal degradation of the product. *Journal of Applied Polymer Science*, *20*(10), 2829–2836. https://doi.org/10.1002/app.1976.070201017

Isogai, A., Saito, T., & Fukuzumi, H. (2011). TEMPO-oxidized cellulose nanofibers. *Nanoscale*, *3*(1), 71–85. https://doi.org/10.1039/C0NR00583E

Katsuura, K., & Mizuno, H. (1966). Flameproofing of cotton fabrics with urea and phosphoric acid in organic solvent. *Sen'i Gakkaishi*, *22*(11), 510–514. https://doi.org/10.2115/fiber.22.510

Klemm, D., Kramer, F., Moritz, S., Lindström, T., Ankerfors, M., Gray, D., & Dorris, A. (2011). Nanocelluloses: A New Family of Nature-Based Materials. *Angewandte Chemie International Edition*, *50*(24), 5438–5466. https://doi.org/10.1002/anie.201001273

Kokol, V., Božič, M., Vogrinčič, R., & Mathew, A. P. (2015). Characterisation and properties of homo- and heterogenously phosphorylated nanocellulose. *Carbohydrate Polymers*, *125*, 301–313. https://doi.org/10.1016/j.carbpol.2015.02.056

Lagier, C. M., Zuriaga, M., Monti, G., & Olivieri, A. C. (1996). Urea-phosphoric acid complex studied by variable temperature 31P NMR spectroscopy and semiempirical calculations. *Journal of Physics and Chemistry of Solids*, *57*(9), 1183–1190. https://doi.org/10.1016/0022-3697(95)00294-4

Lavoine, N., Desloges, I., Dufresne, A., & Bras, J. (2012). Microfibrillated cellulose – Its barrier properties and applications in cellulosic materials: A review. *Carbohydrate Polymers*, *90*(2), 735–764. https://doi.org/10.1016/j.carbpol.2012.05.026

Li, K., Wang, J., Liu, X., Xiong, X., & Liu, H. (2012). Biomimetic growth of hydroxyapatite on phosphorylated electrospun cellulose nanofibers. *Carbohydrate Polymers*, *90*(4), 1573–1581. https://doi.org/10.1016/j.carbpol.2012.07.033

Lim, S., & Seib, P. A. (1993). Preparation and pasting properties of wheat and corn starch phosphates. *Cereal Chemistry*. Retrieved from http://agris.fao.org/agris-search/search.do?recordID=US19940103186

Littunen, K., Snoei de Castro, J., Samoylenko, A., Xu, Q., Quaggin, S., Vainio, S., & Seppälä, J. (2016). Synthesis of cationized nanofibrillated cellulose and its antimicrobial properties. *European Polymer Journal*, *75*, 116–124. https://doi.org/10.1016/j.eurpolymj.2015.12.008

Manet, S. (2007). *Effet de contre-ion sur les propriétés d'amphiphiles cationiques* (Phdthesis, Université Sciences et Technologies - Bordeaux I). Retrieved from https://tel.archives-ouvertes.fr/tel-00250098/document

Montanari, S., Roumani, M., Heux, L., & Vignon, M. R. (2005). Topochemistry of Carboxylated Cellulose Nanocrystals Resulting from TEMPO-Mediated Oxidation. *Macromolecules*, *38*(5), 1665–1671. https://doi.org/10.1021/ma048396c

Mucalo, M. R., Kato, K., & Yokogawa, Y. (2009). Phosphorylated, cellulose-based substrates as potential adsorbents for bone morphogenetic proteins in biomedical applications: A protein adsorption screening study using cytochrome C as a bone morphogenetic protein mimic. *Colloids and Surfaces B: Biointerfaces*, *71*(1), 52–58. https://doi.org/10.1016/j.colsurfb.2009.01.004

Naderi, A., Lindström, T., Weise, C. F., Flodberg, G., Sundström, J., Junel, K., … Runebjörk, A. M. (2016). Phosphorylated nanofibrillated cellulose: production and properties. *Nordic Pulp and Paper Research Journal*, *31*(01), 020–029. https://doi.org/10.3183/NPPRJ-2016-31-01-p020-029

Noguchi, Y., Homma, I., & Matsubara, Y. (2017). Complete nanofibrillation of cellulose prepared by phosphorylation. *Cellulose*, *24*(3), 1295–1305. https://doi.org/10.1007/s10570-017-1191-3

Nuessle, A. C., Ford, F. M., Hall, W. P., & Lippert, A. L. (1956). Some Aspects of the Cellulose-Phosphate-Urea Reaction. *Textile Research Journal*, *26*(1), 32–39. https://doi.org/10.1177/004051755602600105

Ott, E., Spurlin, H. M., Grafflin, M. W., Bikales, N. M., & Segal, L. (1954). *Cellulose and cellulose derivatives*. Interscience Publishers.

Pasqui, D., Rossi, A., Di Cintio, F., & Barbucci, R. (2007). Functionalized Titanium Oxide Surfaces with Phosphated Carboxymethyl Cellulose: Characterization and Bonelike Cell Behavior. *Biomacromolecules*, *8*(12), 3965–3972. https://doi.org/10.1021/bm701033u

Petreus, T., Stoica, B. A., Petreus, O., Goriuc, A., Cotrutz, C.-E., Antoniac, I.-V., & Barbu-Tudoran, L. (2014). Preparation and cytocompatibility evaluation for hydrosoluble phosphorous acid-derivatized cellulose as tissue engineering scaffold material. *Journal of Materials Science: Materials in Medicine*, *25*(4), 1115–1127. https://doi.org/10.1007/s10856-014-5146-z

Reid, J. D., & Mazzeno, L. W. (1949). Preparation and Properties of Cellulose Phosphates. *Industrial & Engineering Chemistry*, *41*(12), 2828–2831. https://doi.org/10.1021/ie50480a039

Reid, J. D., Mazzeno, L. W., & Buras, E. M. (1949). Composition of Two Types of Cellulose Phosphates. *Industrial & Engineering Chemistry*, *41*(12), 2831–2834. https://doi.org/10.1021/ie50480a040

Rol, F., Belgacem, M. N., Gandini, A., & Bras, J. (2018). Recent advances in surface-modified cellulose nanofibrils. *Progress in Polymer Science*. https://doi.org/10.1016/j.progpolymsci.2018.09.002

Rol, F., Karakashov, B., Nechyporchuk, O., Terrien, M., Meyer, V., Dufresne, A., … Bras, J. (2017). Pilot scale twin screw extrusion and chemical pretreatment as an energy efficient method for the production of nanofibrillated cellulose at high solid content. *ACS Sustainable Chemistry & Engineering*. https://doi.org/10.1021/acssuschemeng.7b00630

Saini, S., Yücel Falco, Ç., Belgacem, M. N., & Bras, J. (2016). Surface cationized cellulose nanofibrils for the production of contact active antimicrobial surfaces. *Carbohydrate Polymers*, *135*, 239–247. https://doi.org/10.1016/j.carbpol.2015.09.002

Suflet, D. M., Chitanu, G. C., & Popa, V. I. (2006). Phosphorylation of polysaccharides: New results on synthesis and characterisation of phosphorylated cellulose. *Reactive and Functional Polymers*, *66*(11), 1240–1249. https://doi.org/10.1016/j.reactfunctpolym.2006.03.006

Yajima, S. (2018, August 29). *Announcement regarding expanding lineup of phosphorylated CNF slurry samples*. Retrieved from https://www.ojiholdings.co.jp/Portals/0/resources/content/files/english/ir/news/2018/WCd2Wuj.pdf

Yurkshtovich, N. K., Yurkshtovich, T. L., Kaputskii, F. N., Golub, N. V., & Kosterova, R. I. (2007). Esterification of viscose fibres with orthophosphoric acid and study of their physicochemical and mechanical properties. *Fibre Chemistry*, *39*(1), 31–36. https://doi.org/10.1007/s10692-007-0007-x